

Figure 3. Three model simulations of (a) measured global mean temperature and (b) the temperature difference between hemispheres. The most inclusive simulation (orange curves) is driven by changing concentrations of CO, and other greenhouse gases, changing solar irradiation, and other forcing agents discussed in the text. The other two simulations branch off at 17 kyr.

One (yellow) considers only subsequent greenhouse-gas changes, and the other (blue) considers only changes in solar irradiation. (Adapted from ref. 1.)

as it appears to have done about 19 kyr ago, the southern hemisphere retains much of the heat that it normally ships north. The most plausible explanation for that weakening is the recession of ice sheets in and near the far North Atlantic during the gradual warming of the preceding three millennia. Excessive melting in the north inhibits the AMOC because the less dense, low-salinity meltwater sinks less readily to form the southward deep current that's needed to complete the thermohaline circuit.

Simulations

To assess the validity and relative importance of the various mechanisms adduced to explain the last deglaciation, Shakun and company used a National Center for Atmospheric Research climate model to simulate the temperature record for the period from 22 to 7 kyr ago

with three different suites of inputs and driving mechanisms. Figure 3 shows the simulation results for the global mean temperature and the mean-temperature difference between the hemispheres.

The most inclusive simulation, shown by the orange curves, is driven by the measured record for CO₂ and other greenhouse gases, the calculated changes of solar irradiation at various latitudes due to orbital and axial cycles, the measured ice-sheet coverage, and estimates of freshwater fluxes from melting ice sheets. The other two simulations branch off the inclusive one at 17 kyr. The yellow curves consider only subsequent changes in the greenhouse-gas concentrations, and the light-blue curves consider only changes in solar irradiation.

The inclusive simulation fits the global and hemisphere-difference temperature records quite well. But so, in broad

strokes, does the greenhouse-only simulation—except for the short-term wiggles attributed to AMOC interruption. By contrast, the solar-only simulation yields only a small fraction of the steep global warming that started at about 17 kyr. "So on that time scale," says Shakun, "it seems clear that CO₂ was the principal driver." The simulations don't try to reproduce the CO₂ rise; it's simply taken as an input. "That's because we don't yet understand in sufficient detail how the CO₂ took off so abruptly at 17.5 kyr," he explains.

The likely trigger

Although rising CO_2 seems to have been the driving force of the last deglaciation after that takeoff, the team concludes that it probably was not the initial trigger. After all, global temperature had been rising steadily, if slowly, since 21.5 kyr, with a slight steepening at 19 kyr, just when the AMOC started weakening.

Exploiting their unique temperatureproxy database covering all latitudes in the early millennia of the deglaciation, Shakun and company tentatively offer the following trigger scenario: Starting around 22 kyr ago, gradually increasing summer insolation at high northern latitudes—due to increasing axial tilt and the precession of the June solstice toward perihelion—began melting enough ice to start disrupting the AMOC by 19 kyr. As the AMOC's northward heat transport continued to weaken, the consequent warming of the carbon-rich Southern Ocean could have unleashed the steep ascent of CO₂ concentration that took over and accelerated the global warming some 1500 years later.

Bertram Schwarzschild

Reference

1. J. D. Shakun et al., Nature 484, 49 (2012).

Classical vortex beams show their discrete side

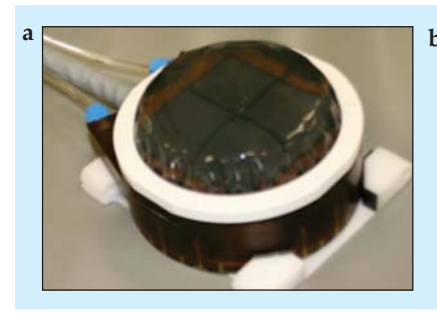
Researchers twist sound, testing a fundamental law of the quantization of orbital angular momentum.

aced with danger, the Doctor, protagonist of the science fiction television series *Doctor Who*, often availed himself of a tool known as a sonic screwdriver. A bit larger than an ink pen, the sonic screwdriver was, among other things, a lock pick, a remote control, and an alien-detection device. The Doctor's tool was fictional, of course, but now Michael MacDonald and colleagues at the University of

Dundee in the UK, in collaboration with Gabriel Spalding of Illinois Wesleyan University, have developed a real-life sonic screwdriver—an ultrasound device capable of generating high-angular-momentum acoustic vortices. With it, they've obtained an elusive measurement of the ratio of orbital angular momentum (OAM) to energy in a vortex beam.¹

The notion that propagating waves

can possess OAM is just 20 years old. First advanced by Les Allen and coworkers for the specific case of electromagnetic waves, the conclusion follows from the observation that a light beam's momentum is always perpendicular to its wavefront. A beam having a helical wavefront should therefore have some OAM about its axis, and a beam made up of several intertwined helical wavefronts should have even more. Each photon, Allen and his colleagues asserted, must have OAM of *lh*, where the integer *l* is the topological



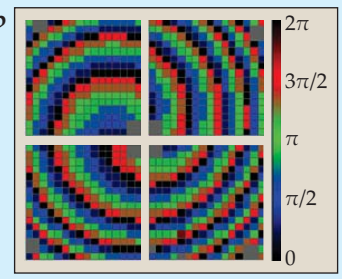


Figure 1. Sound with a twist. (a) Dubbed a sonic screwdriver, the ultrasound device shown here, roughly 10 cm across, contains a 32×32 array of individually addressable transducers. The relative phases of the transducers can be adjusted to customize the shape of an acoustic wave. **(b)** With this phase profile, for instance, the array would generate a beam of three intertwined helical wavefronts. (Images courtesy of Gabriel Spalding.)

charge—essentially, the number of intertwined helices—and \hbar is the reduced Planck's constant.

Experiments leave little doubt that helical topology does indeed endow a propagating wave with OAM. (See the article by Miles Padgett, Johannes Courtial, and Les Allen in PHYSICS TODAY, May 2004, page 35.) Such waves have come to be known as vortex beams and have given rise to, for example, the optical wrench, a special form of optical tweezer that can simultaneously trap and torque a small dielectric particle. OAM is now also known to be a property of acoustic and electron vortex beams.

And there's little reason to suspect that the OAM carried by any vortex beam's constituent particles—be they photons, phonons, or the like—could be

different than $l\hbar$ or, equivalently, that the ratio of any beam's total OAM to its energy, L/E, could be different than l/ω , where ω is the angular frequency. Rigorous analysis of specific propagatingwave solutions seems to show as much.^{2,3} Plus, that picture meshes neatly with the broader paradigm of quantum mechanics. Still, experimental confirmation has proved challenging.

In essence, the experiment calls for simultaneously measuring the radiation pressure and torque exerted by a vortex beam on a target. From the radiation pressure, one obtains the energy flux; from the torque, the flux of OAM. One difficulty with optical beams, however, is that they must be focused tightly over a short distance to hold their target—typically a micron-sized or smaller particle—in place on the beam axis. The

resulting wide range of incidence angles severely complicates measurement of the radiation pressure. By contrast, acoustic forces are often strong enough to be measured against macroscopic objects, which can be held in place by more convenient means.

Putting twists in an acoustic wave, however, is no trivial matter. Acoustic beams must typically be shaped by coordinating the phases of multiple point sources to give a desired superposition. As a result, generating even a single helical wavefront is a formidable task, and ideally, one would also want to check the theory for cases in which several helices are intertwined. Previously, the benchmark for acoustic vortex beams had been, at most, two intertwined helical wavefronts generated with a half dozen transducers. The

50 Years in the Making. . . DSP^{EC}-50.

Advanced, Fourth Generation ORTEC DSP-Based Gamma-Ray Spectrometer for Germanium Detectors.

DSPEC-50 salutes the 50th year in which ORTEC has delivered innovative and quality nuclear instrumentation to scientists in a broad range of applications worldwide. The new DSPEC-50 brings together 50 years of design experience and innovation skills of our developers.

In introducing the DSPEC-50, ORTEC has launched an all-new digital instrument platform, enhanced with a number of unique features and modes of operation which have distinct benefit in real-world applications.

Advanced DSP Algorithms Ensure Enhanced Spectroscopic Performance

- ZDT "loss free" dead-time correction.
- Low frequency noise rejection filter (LFR).
- Charge trapping correction.
- · Enhanced throughput mode.

For more information, see: www.ortec-online.com/download/DSPEC-50.pdf

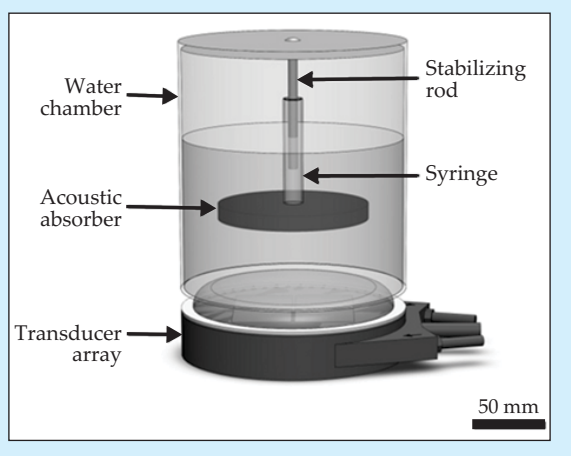
801 South Illinois Ave., Oak Ridge, TN 37831-0895 U.S.A. • (865) 482-4411 • Fax (865) 483-0396 • ortec.info@ametek.com
For International Office Locations, Visit Our Website

Dundee team's sonic screwdriver, pictured in figure 1, features an array of more than 1000 individually addressable ultrasound transducers and can

generate beams with up to 12 intertwined helices.

In the team's experimental setup, depicted in figure 2, the transducer

Figure 2. The experimental setup. The energy and orbital angular momentum of the acoustic beam emitted by a transducer array reveal themselves in the mechanical response of a sound-absorbing disk: The disk levitates by a distance related to the beam energy and rotates at a speed related to the orbital angular momentum. An air-filled syringe, free to slide vertically along the stabilizing rod, helps to buoy the disk and prevent it from tilting. (Adapted from ref. 1.)



array directs a vortex beam upward toward a sound-absorbing disk submersed in a water chamber. The rising vortex lifts the disk by a distance related to *E* and spins it at a rate related to *L*. In the end, OAM theory emerged from the experiment unscathed: The measured ratio *L/E* plotted against *l* agreed with predictions to well within experimental error. With one case now closed, the researchers look to use the sonic screwdriver to design nondiffracting Bessel beams and other complex beam shapes that could prove useful for ultrasound surgery.

Ashley G. Smart

References

- 1. C. E. M. Demore et al., *Phys. Rev. Lett.* **108**, 194301 (2012).
- 2. L. Allen et al., Phys. Rev. A 45, 8185 (1992).
- 3. L. Zhang, P. L. Marston, *Phys. Rev. E* **84**, 065601 (2011).

Time to reset isotopic clocks?

Two new studies revise key parameters in radiometric dating.

ust as radiocarbon dating gives the ages of once-living materials up to tens of thousands of years old, longer-lived radioisotopes are used to date rocks that are millions or billions of years old. Now, two wrenches have been thrown into the works. Joe Hiess and colleagues of the British Geological Survey have found that the ratio of uranium-238 to uranium-235 varies more than anyone previously thought it did, or could. The result has a small but significant effect on the widely used uranium-lead dating scheme. And a team

of researchers led by Michael Paul (Hebrew University in Jerusalem) and Takashi Nakanishi (Kanazawa University, Japan) measured the half-life of samarium-146 to be 35% less than the currently accepted value.² Samarium-146 dating is of more limited applicability, but if the new measurement is upheld, it means a major revision in all the dates derived from it.

Uranium

Uranium's two long-lived isotopes, ²³⁵U and ²³⁸U, decay through a series of

The Fish Canyon Tuff in Colorado formed in a massive volcanic eruption 28.5 million years ago. Two mineral samples from the site—one of zircon, one of titanite—have uranium isotopic ratios that differ by almost 5 parts per thousand.

alpha and beta emissions into ²⁰⁷Pb and ²⁰⁶Pb, respectively. Uranium–lead dating is usually done on minerals, such as zircon, that can incorporate U impurities into their crystal lattices but that strongly reject Pb. If no Pb was present in the mineral when it first formed, any Pb found in it later must be radiogenic. Knowing U's half-life and measuring the relative amounts of U and Pb thus gives the age of the mineral.

That two U isotopes decay into Pb with different half-lives (704 million years for ²³⁵U and 4.47 billion years for ²³⁶U) offers a valuable double check: The ²³⁵U–²⁰⁷Pb age should agree with the ²³⁸U–²⁰⁶Pb age. The redundancy also provides a convenient shortcut. If the ²³⁸U/²³⁵U ratio is already known, then ages can be calculated through measurements of Pb isotopes alone. That Pb–Pb dating is typically used with samples older than about a billion years.

It's long been assumed that the present ²³⁸U/²³⁵U ratio should be the same everywhere on Earth: The mass difference between the two isotopes was presumed to be too small to affect their behavior in natural geological processes. Standard Pb–Pb dating protocol uses a ²³⁸U/²³⁵U ratio of 137.88 with zero uncertainty. But several recent studies have cast doubt on that number.³ Some have suggested, based on analysis of U ores, that it should be closer to 137.80, and others have found that it might not even be constant.

To examine the issue systematically, Hiess and colleagues looked at 58